IOP Publishing Superconductor Science and Technology
Supercond. Sci. Technol. 31 (2018) 065004 (5pp) https://doi.org/10.1088/1361-6668/aabb4c

Carrier doping into a superconducting $BaPb_{0.7}Bi_{0.3}O_{3-\delta}$ epitaxial film using an electric double-layer transistor structure

S Komori[1] and **I Kakeya**

Department of Electronic Science and Engineering, Kyoto University, Katsura, Nishikyo-ku, Kyoto 615-8510, Japan

E-mail: komori@sk.kuee.kyoto-u.ac.jp

Received 28 January 2018, revised 24 March 2018
Accepted for publication 3 April 2018
Published 27 April 2018

Abstract

Doping evolution of the unconventional superconducting properties in $BaBiO_3$-based compounds has yet to be clarified in detail due to the significant change of the oxygen concentration accompanied by the chemical substitution. We suggest that the carrier concentration of an unconventional superconductor, $BaPb_{0.7}Bi_{0.3}O_{3-\delta}$, is controllable without inducing chemical or structural changes using an electric double-layer transistor structure. The critical temperature is found to decrease systematically with increasing carrier concentration.

Keywords: EDLT, high temperature superconductivity, $BaBiO_3$

(Some figures may appear in colour only in the online journal)

1. Introduction

Several $BaBiO_3$-based compounds show three-dimensional high temperature superconductivity, whose critical temperature T_c, is much higher than that expected from their low carrier density. $Ba_{1-x}K_xBiO_{3-\delta}$ (BKBO) and $BaPb_{1-x}Bi_xO_{3-\delta}$ (BPBO) are two such compounds that show T_c's of 30 K [1] and 13 K [2], respectively, with carrier concentrations as low as 2×10^{21} cm^{-3} [3, 4]. The origin of their superconductivity is still open to much debate. Besides their low carrier concentration, $BaBiO_3$-based superconductors and cuprate superconductors share several similarities such as the existences of metal–insulator transition [5, 6], pseudogap phase [7, 8], and charge density wave (CDW) [8–10]. The relationship between these phenomena and the high temperature superconductivity they exhibit has been the subject of intensive study for several decades. The key to revealing these relationships is to understand the complex doping evolution of electric structures. In BKBO and BPBO, doping evolutions have been mainly studied by changing their chemical composition, x [1–6]. Although a decrease in K^+ and Pb^{4+} ions in BKBO and BPBO apparently seems to increase the number of electron carriers which will form Cooper pairs in the superconducting state, an increase in δ caused by charge compensation generates the CDW order and localizes electrons to the Bi site [11, 12]. This has been reported both in single crystals [13] and thin films [14]. The typical δ value of $BaBiO_{3-\delta}$ without K^+ and Pb^{4+} is around 0.5 [15] and it is known as a CDW insulator. Since a change in the chemical composition results in a corresponding change in both the carrier concentration and δ, the direct relationship among the carrier concentration, the CDW order and the superconducting properties has not been clarified in detail in $BaBiO_3$-based compounds.

In BPBO, the electron carrier concentration increases with increasing x and T_c becomes a maximum at $x = 0.3$ [2]. Increasing x beyond 0.3 leads to an increase in δ (and the CDW order), and a decrease in T_c. It has been reported that single-crystal BPBO is structurally dimorphic in the superconducting region ($x = 0.15$–0.35) and composed of phases with orthorhombic and tetragonal structures [16]. The tetragonal phase is believed to be responsible for the superconductivity because its volume fraction becomes maximum at optimally-doped region ($x = 0.3$) [16, 17]. However, the origin of the T_c-peak at $x = 0.3$ and how the carrier concentration affects T_c have not been fully understood yet.

[1] Author to whom any correspondence should be addressed.

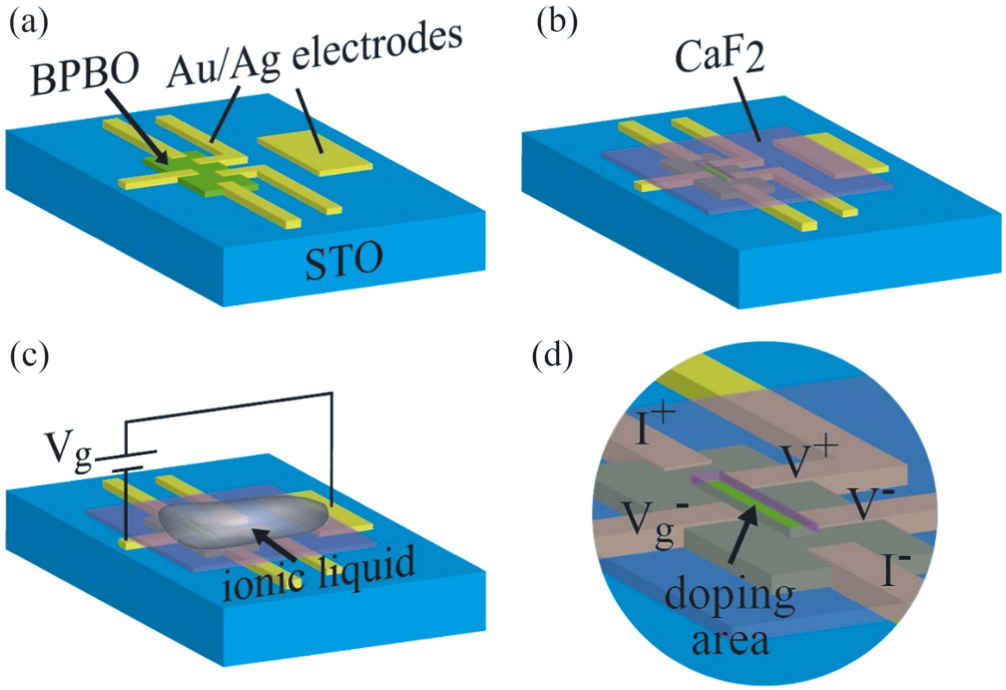

Figure 1. Schematic illustration of the device used in this work. (a) Patterned BPBO epitaxial film with Au/Ag electrodes. (b) The device after CaF_2 deposition. (c) The final structure of the device. The ionic liquid was placed over both the gate electrode and BPBO. (d) Enlarged illustration of the device structure around BPBO. On BPBO, there is an area which is not covered by CaF_2 to form the contact between BPBO and the ionic liquid.

In this work, we have carried out the electron doping for an optimally-doped superconducting BPBO epitaxial film with $x = 0.3$ using electric double-layer transistor (EDLT) structure [18–20] and investigated the relation between the T_c and the carrier concentration without changing the chemical composition. The maximum carrier concentration achieved by the doping is $3 \times 10^{22}\,\mathrm{cm}^{-3}$, which is higher by an order of magnitude than that without the doping.

2. Experimental

A $BaPb_{0.7}Bi_{0.3}O_{3-\delta}$ (BPBO) epitaxial film was grown on an $SrTiO_3$ (100) substrate with an RF-magnetron sputtering system, which is generally used to grow $BaBiO_3$-based superconductors [4, 14, 21]. The substrate temperature was 650 °C and the atmosphere was 100 mTorr of the mixed gas of Ar:50% and O_2:50%. The cathode voltage was 1.4 kV. The approximate deposition rate was $30\,\mathrm{nm\,min}^{-1}$ and the total thickness of the film was 610 nm. After the deposition, the film was patterned into the size of $500 \times 100\,\mu\mathrm{m}^2$ by laser lithography and an Ar ion milling technique. Subsequently, Au (50 nm)/Ag (15 nm) electrodes were fabricated by electron beam deposition and the lift-off technique, as shown in figure 1(a). Since the contact resistance of Ag/BPBO is much lower than that of Au/BPBO, Ag was deposited on BPBO first. To avoid an electro-chemical reaction of Ag and the ionic liquid, Au was subsequently deposited on Ag/BPBO. The electrodes around BPBO were covered by an insulating CaF_2 (200 nm) film to apply the electric field only on BPBO as represented in figure 1(b). The ionic liquid used in this work is DEME-TFSI (Kanto Chemical). At room temperature, the ionic liquid was placed over the BPBO and the gate electrode as illustrated in figure 1(c). The gate voltage, V_g, was applied in the range of ±2 V to avoid inducing oxygen deficiencies due to the electro-chemical reactions. The carrier concentration and T_c controlled in this range were reversible. The transport properties of the device were measured by the physical properties measurement system. We found that the evacuation of air before cooling causes a dispersion of the ionic liquid, so low temperature measurements were performed under the ambient pressure of helium gas. The Hall carrier density was determined by a linear fit to the transverse resistivity as a function of the out-of-plane external magnetic field in the range of ±5 T.

3. Results and discussion

To confirm the ideal crystallinity and the roughness of a BPBO epitaxial film, we collected and analyzed its x-ray diffraction patterns and atomic force microscope images. High resolution x-ray diffraction patterns confirmed the single orientation of BPBO with rocking curves on the (001), (002) and (003) Bragg peaks showing full width at half maximum values of 0.72°, 0.73°, and 0.56°, respectively; see figure 2(a). The c-axis lattice constant was determined to be 4.28 Å, which is consistent with the value obtained from the high resolution diffraction experiment for polycrystalline BPBO with $x = 0.3$ [22]. Figure 2(b) shows a typical atomic force microscope image of the BPBO film indicating an atomically

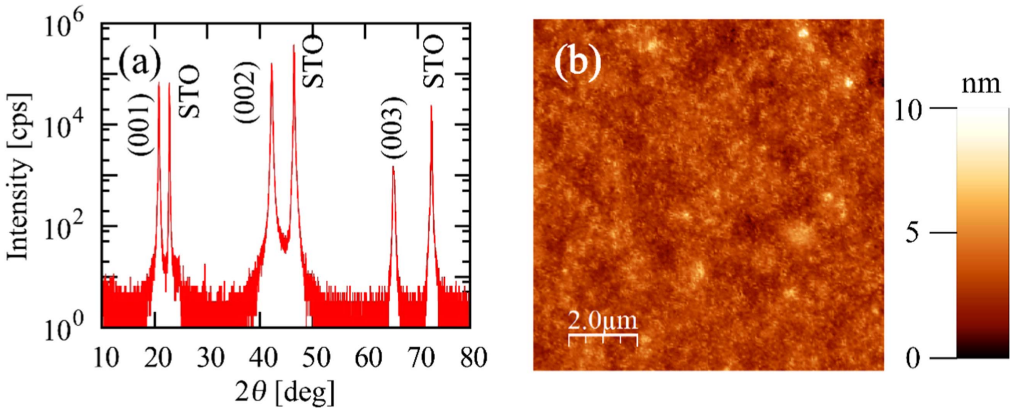

Figure 2. (a) θ–2θ x-ray diffraction pattern of BPBO on STO (001). (b) Atomic force microscope image of a BPBO epitaxial film.

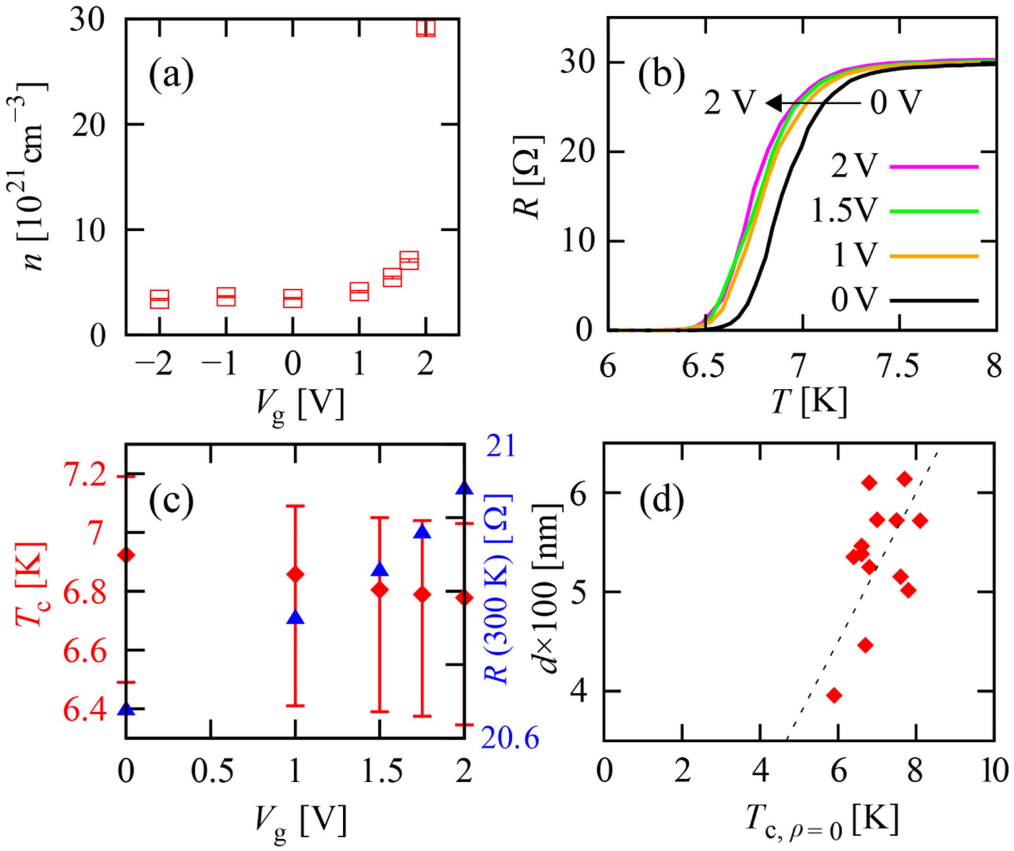

Figure 3. Gate voltage dependence of (a) Hall carrier concentration at 300 K, (b) resistance, (c) critical temperature (left axis, red diamonds), and room temperature resistance (right axis, blue triangles). The critical temperatures were extracted from 50% of the resistive transition. The vertical error bars for the critical temperatures show the width of the transition (from $T_{c,onset}$ to zero resistivity critical temperature, $T_{c,\rho=0}$). (d) Relation between the thickness and the critical temperature of BPBO epitaxial films. The dashed line is a guide to the eye.

flat surface with a root mean square roughness of about 1 nm over an area of 100 μm^2.

The Hall carrier density n, at 300 K with different V_g for the BPBO film is shown in figure 3(a). Although one might point out that Hall coefficient is not a direct measure of n for dimorphic BPBO, we assumed its homogeneous transport properties. The increase of n with increasing V_g indicates the carrier doping effect through EDLT. As shown in figure 4(a), anions in the ionic liquid accumulate around the positively biased gate electrode whereas cations accumulate around the negatively biased BPBO, which in turn results in the accumulation of electrons at the surface of BPBO. The change of the V_g from 0 to +2 V changes the carrier density of BPBO by an order of magnitude. Although positive V_g significantly affects n, negative V_g does not; this is because the carrier doping is not effective for the entire film, but only for the part of the film around the surface. The increase in the carrier density of the BPBO in the carrier doping region is observable through the decrease of its Hall resistivity. However, the decrease in the carrier density cannot be observed because

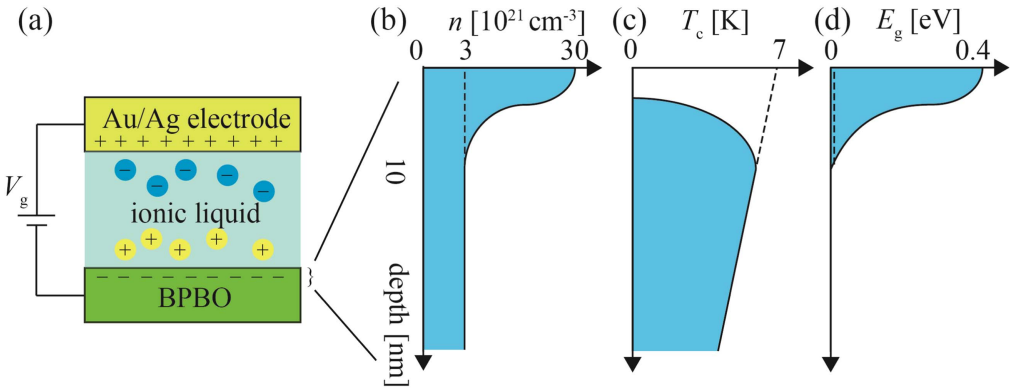

Figure 4. (a) Schematic diagram of the EDLT structure on BPBO. Depth profiles of (b) critical temperature, (c) electron concentration, and (d) CDW energy gap at around the surface of BPBO at $V_g = 2$ V. The dashed lines show the profiles for $V_g = 0$.

of the lower Hall resistivity in the rest part of the BPBO film that has a higher carrier concentration.

The temperature dependence of the resistivity around T_c with various V_g is shown in figure 3(b). It was found that T_c decreases and resistance increases with increasing V_g (carrier concentration), as plotted in figure 3(c). Here, T_c was defined by 50% of the resistive transition. A change of V_g from 0 to +2 V results in a decrease in T_c by 150 mK and an increase in the room temperature resistance by 1.5%. These changes were reversible, which rules out affects from any deteriorations of the film such as induction of oxygen deficiencies. Decrease in T_c is not easily observable in a superconductor which is thicker than the carrier doping layer because the T_c-suppression does not occur in the remaining part of the film under the carrier doping layer. However, in our device, the T_c-suppression is observable due to a large T_c-gradient in the film, even when the film is much thicker than the carrier doping layer. Since BPBO has a long coherence length ($\xi(0) = 7$ nm [4]) compared with cuprate superconductors ($\xi_c(0) = 0.3$–0.4 nm for $YBa_2Cu_3O_7$ [23] and $\xi_c(0) \sim 0.1$ nm for Bi-based cuprates[24]), its superconductivity is sensitive to impurities and strain in epitaxial films. Therefore, even in the 610 nm-thick film which was used in this work, T_c is much lower than that of single crystals. T_c of BPBO epitaxial films gradually increases with increasing thickness as shown in figure 3(d). This is considered to be due to a gradual decrease in the density of crystal defects caused by the strain in epitaxial films. The low-T_c region near the BPBO/STO interface can be proximitized by high-T_c region near the surface which has relatively high carrier concentration. This can also result in a T_c-gradient in epitaxial films.

The 1.5% increase in the resistance by the application of $V_g = +2$ V can be translated to an appearance of the highly resistive carrier doping layer with the thickness of 9 nm (1.5% of the total 610 nm). The 1.5% resistance shift was observed down to the onset temperature of the superconducting transition $T_{c,onset}$, suggesting that the thickness of the carrier doping layer does not depend strongly on the temperature. This can be due to the small change (10%) of the Hall carrier concentration between room temperature and $T_{c,onset}$ in BPBO ($x = 0.3$) epitaxial films [4]. The linear suppression of T_c with increasing V_g despite the nonlinear increase in the carrier concentration implies the nonlinear relation between the carrier concentration and the thickness of the doping layer. The thickness of the carrier doping layer is determined by the charge screening length, which depends on the carrier concentration, dielectric constant, and effective mass of materials. A typical charge screening length for semiconductors is few nanometers, which corresponds to the length scale of the band bending effect at the surface of semiconductors. The carrier doping layer of 9 nm estimated for BPBO in this work is longer than the typical charge screening length. However, it is worth noting that in some doped Mott insulators such as VO_2 [25], $NdNiO_3$ [26], and $Pr_{1-x}Sr_xMnO_3$ [27], the charge screening length of several tens of nanometers has been reported. This is considered to be due to the metal–insulator transition at the interface induced by the carrier doping. Since the electric states of a metallic phase and an insulating phase are significantly different, energy band structures of the bulk and surface becomes discontinuous by the carrier doping. The energy band structure of the surface is gradually relaxed to that of the bulk and this relaxation length is considered to be longer than the charge screening length. This can enable the long-range control of the electronic state by EDLT in Mott insulators including BPBO.

Finally, we discuss the details of the carrier doping effect in the BPBO epitaxial film. The carrier concentration of BPBO at $x = 0$ is as low as 3×10^{20} cm^{-3} due to a small amount of the density of states at the Fermi level in Pb(6s)-O (2p) hybrid bands. Substitution of $Bi^{4+}(6s)^1$ for $Pb^{4+}(6s)^0$ (i.e., increasing x) results in electron doping and an increase in T_c until $x = 0.3$ [4]. However, the resistivity increases with increasing x [4, 28]. This is explained by the formation of CDW order in which BiO_6 octahedra exhibit breathing distortions. The energy gap of the CDW insulating order increases with increasing x (δ) and results in the suppression of T_c at $x > 0.3$. Eventually, the superconductivity disappears at around x = 0.35 ($\delta = 0.18$) [4, 28]. In this work, electron doping for the sample with $x = 0.3$ was found to decrease T_c as illustrated in figures 4(b) and (c). In addition, a decrease in

the resistivity was not observed in spite of the significant increase in the carrier concentration. In high temperature cuprate superconductors, an increase in n by an order of magnitude drastically decreases their resistivity. In $La_{2-x}Sr_xCuO_4$, an increase in n from 3×10^{21} to $3 \times 10^{22}\,cm^{-3}$ observed in this work corresponds to a change from $x = 0.13$ (slightly underdoped) to $x = 0.25$ (highly overdoped) [29], which reduces the resistivity by a factor of 3 [30]. Here, the Sr concentration x corresponds to the effective number of holes per Cu atom in the CuO_2 superconducting layer. However, in this work, the resistivity of the BPBO film was not decreased but increased by 1.5%, suggesting that the surface of the BPBO film became more resistive due to the electron doping. This trend is similar to the Bi substitution effect that increases both the carrier concentration and the resistivity. The most plausible interpretation of the results in this work is that the electron doping into Bi^{5+} ions has increased the concentration of Bi^{3+} ions and led to an enhancement of the CDW order which is generated by an alternating array of Bi^{3+} and Bi^{5+} ions. In BPBO, it has been reported that the CDW energy gap E_g [eV] roughly follows $E_g = 0.7x - 0.3$ [31]. Application of $V_g = 1.75$ V increased the carrier concentration of the device to $8 \times 10^{21}\,cm^{-3}$, which is the value for $BaBiO_3$ ($x = 1$). This allows for the generation of a CDW gap of 0.4 eV (the value for $x = 1$) as illustrated in figure 4(d) and leads to an increase in the normal state resistivity. Considering the fact that the Bi substitution for $x = 0.3$ film increases E_g and suppresses T_c, it is highly possible that the T_c-suppression observed in this work is due to the formation of the CDW order.

4. Conclusions

We have observed the carrier doping effect in a $BaBiO_3$-based unconventional superconductor by using an EDLT structure for the first time. An increase in the electron doping level from 3×10^{21} to $3 \times 10^{22}\,cm^{-3}$ was observed in a $BaPb_{0.7}Bi_{0.3}O_{3-\delta}$ epitaxial film. It was found that the increase in the carrier concentration results in the suppression of the superconductivity and the increase in the normal state resistivity. T_c-decrease of 150 mK and 1.5%-increase in the room temperature resistivity were observed in the 610 nm-thick film.

Acknowledgments

The authors deeply thank Y Matsumoto, Y Kamei, A Uzawa, Y Nakagawa and M Suzuki for experimental support and fruitful discussions. This work was financially supported by the JSPS KAKENHI Grant No.15J07623.

ORCID iDs

S Komori https://orcid.org/0000-0002-8288-6786

References

[1] Cava R J, Batlogg B, Krajewski J J, Farrow R, Rupp L W J, White A E, Short K, Peck W F and Kometani T 1988 *Nature* **332** 814–6
[2] Sleight A W, Gillson J L and Bierstedt P E 1975 *Solid State Commun.* **17** 27–8
[3] Hellman E S and Hartford E H Jr 1993 *Phys. Rev.* B **47** 11346–53
[4] Suzuki M 1993 *Japan. J. Appl. Phys.* **32** 2640–7
[5] Khosroabadi H, Miyasaka S, Kobayashi J, Tanaka K, Uchiyama H, Baron A Q R and Tajima S 2011 *Phys. Rev.* B **83** 224525
[6] Namatame H, Fujimori A, Takagi H, Uchida S, de Groot F M F and Fuggle J C 1993 *Phys. Rev.* B **48** 16917–25
[7] Namatame H, Fujimori A, Torii H, Uchida T, Nagata Y and Akimitsu J 1994 *Phys. Rev.* B **50** 13674–8
[8] Tajima S, Uchida S, Masaki A, Takagi H, Kitazawa K and Tanaka S 1987 *Phys. Rev.* B **35** 696–703
[9] Le T M, Bosak A, Souliou S M, Dellea G, Loew T, Heid R, Bohnen K, Ghiringhelli G, Krisch M and Keimer B 2014 *Nat. Phys.* **10** 52–8
[10] Du C-H and Hatton P D 1995 *Europhys. Lett.* **31** 145–50
[11] Balzarotti A, Menushenkov A, Motta N and Purans J 1984 *Solid State Commun.* **49** 887–90
[12] Anderson P W 1975 *Phys. Rev. Lett.* **34** 953–5
[13] Idemoto Y, Iwata Y and Fueki K 1992 *Physica* C **201** 43–9
[14] Suzuki M and Murakami T 1985 *Solid State Commun.* **53** 691–4
[15] Hashimoto T, Kobayashi T, Tanaka H, Hirasawa R, Hirai H and Tagawa H 1998 *Solid State Ion.* **108** 371–6
[16] Climent-Pascual E, Ni N, Jia S, Huang Q and Cava R J 2011 *Phys. Rev.* B **83** 174512
[17] Marx D T, Radaelli P G, Jorgensen J D, Hitterman R L, Hinks D G, Pei S and Dabrowski B 1992 *Phys. Rev.* B **46** 1144–57
[18] Ueno K, Nakamura S, Shimotani H, Ohtomo A, Kimura N, Nojima T, Aoki H, Iwasa Y and Kawasaki M 2008 *Nat. Mater.* **7** 855–8
[19] Shimotani H, Asanuma H, Tsukazaki A, Ohtomo A, Kawasaki M, Shimotani H, Asanuma H, Tsukazaki A and Ohtomo A 2010 *Appl. Phys. Lett.* **91** 82106
[20] Bollinger A T, Dubuis G, Yoon J, Pavuna D, Misewich J and Bozovic I 2011 *Nature* **472** 458–60
[21] Iyori M, Suzuki S, Suzuki H, Yamano K, Takahashi K, Usuki T, Yoshisato Y and Nakano S 1993 *Japan. J. Appl. Phys.* **32** 1946–51
[22] Sleight A W 2015 *Physica* C **514** 152–65
[23] Welp U, Kwok W, Crabtree G, Vandervoort K and Liu J 1989 *Phys. Rev. Lett.* **62** 1908–11
[24] Matsushita T 1993 *Physica* C **205** 289–95
[25] Nakano M, Shibuya K, Okuyama D, Hatano T, Ono S, Kawasaki M, Iwasa Y and Tokura Y 2012 *Nature* **487** 459–62
[26] Asanuma S *et al* 2015 *Appl. Phys. Lett.* **97** 142110
[27] Hatano T, Ogimoto Y, Ogawa N, Nakano M, Ono S, Tomioka Y, Miyano K, Iwasa Y and Tokura Y 2013 *Sci. Rep.* **3** 2904
[28] Uchida S, Kitazawa K and Tanaka S 1987 *Phase Transit.* **8** 95–128
[29] Padilla W J, Lee Y S, Dumm M and Blumberg G 2005 *Phys. Rev.* B **72** 60511
[30] Boebinger G, Ando Y, Passner A, Kimura T, Okuya M, Shimoyama J, Kishio K, Tamasaku K, Ichikawa N and Uchida S 1996 *Phys. Rev. Lett.* **77** 5417–20
[31] Uwe H, Minami H, Nishio T, Ahmad J and Shizuya M 2007 *Ferroelectrics* **346** 1–9